

Infeed Control Algorithm of Sorting System Using Modified Trapezoidal Velocity Profiles

Ki Hak Kim, Yong Hoon Choi, and Hoon Jung

This paper applies acceleration/deceleration control-based velocity profiles to an infeed control algorithm for a cross-belt-type sorting system to improve the accuracy and performance of the system's infeed. The velocity profiles are of a trapezoidal shape and often have to be modified to ensure that parcels correctly synchronize with their intended carriers. Under the proposed method, an infeed line can handle up to 5,600 items/h, which indicates a 40% increase in performance in comparison with its existing handling rate of 4,000 items/h. This improvement in performance may lead to a reduction in the number of infeed lines required in a sorting system. The proposed infeed control algorithm is applied to a cross-belt-type sorting system (model name: SCS 1500) manufactured by Vanderlande Industries.

Keywords: Velocity profile, sorting system, infeed control, cross-belt sorter, acceleration/deceleration control, E-tray sorter, trapezoidal velocity profile.

I. Introduction

Recently, parcel volumes have been increasing year upon year, and this has meant that the parcel delivery service industry has had to expand to keep up with demand. As a result, more and more mail or distribution centers are turning towards the use of parcel sorting systems to efficiently sort parcels. Nowadays, sorting machines such as the cross-belt and E-Tray have been developed and commercialized to increase a sorting system's maximum capacity and its ability to handle all sizes of parcels. In particular, the E-tray- and cross-belt-type sorting machines have been developed and used in such a way so as to provide sorting systems employing these devices with an overall performance of 10,000 or more items/h. However, since the *track* speed of a parcel sorting system can be up to 2.5 m/s or more, it is difficult to accurately input parcels to track carriers (or trays). Therefore, the infeed control in a sorting system is a demanding technical control task and an essential factor for the optimization of a sorting system.

The infeed of a sorting system is usually controlled using one of two methods. The first method usually involves the halting of all of the system's variable control belts (VCBs) when either track carriers are unavailable or it is not possible to synchronize a parcel with a carrier, whereas the other is to control the VCBs' rates of acceleration or deceleration so as to maintain the availability of track carriers and thus reduce the number of times the system has to temporarily come to a complete halt. Low-performance sorters, such as a mechanical tilt tray and slide-shoe, use the former, whereas high-performance sorters, such as the cross-belt sorter and E-tray sorter, use the latter.

To make sure that a load can be moved to a specified position at a specified time along the infeed line, it is necessary to design the desired velocity profiles of the infeed's VCBs

Manuscript received Aug. 7, 2014; revised Feb. 3, 2015; accepted Feb. 6, 2015.

This work was supported by the Postal Technology R&D program of MSIP (10039146, Development of Implementation Technology for SMART Post).

Ki Hak Kim (corresponding author, kkh8166@etri.re.kr), Yong Hoon Choi (ychoi@etri.re.kr), and Hoon Jung (hoonjung@etri.re.kr) are with the IT Convergence Technology Research Laboratory, ETRI, Daejeon, Rep. of Korea.

beforehand [1]–[9]. One of the most commonly used velocity profiles is that of a trapezoidal velocity profile [10]–[12]. It includes the following three parts: constant acceleration, constant velocity, and constant deceleration. However, to improve the efficiency of a high-speed sorting system and to ensure that parcels synchronize correctly with their intended carriers, it is often necessary to use modified trapezoidal velocity profiles. In Section II, we explain how the infeed control process works in terms of how parcels on conveyor belts and track carriers are synchronized. Then, in Section III, we show when it is necessary to apply a modified trapezoidal velocity profile and the reasons for doing so. Finally, the proposed infeed control algorithm is implemented in a cross-belt-type sorting system (model name: SCS 1500) manufactured by Vanderlande Industries [13].

II. Typical Trapezoidal Velocity Profile

As shown in Fig. 1, the velocity profile shown has a trapezoidal shape, which consists of ramp-up, steady, and ramp-down parts. A trapezoidal velocity profile can be basically obtained from the relation among a position, velocity, and acceleration.

Figure 2 shows the trapezoidal velocity profiles for three distinct cases; that is, when the total movement distance, D_{total} , is greater than the sum of the total movement distance covered under both the acceleration segment (a_{total}) and the deceleration segment (d_{total}) (that is, when $D_{\text{total}} > a_{\text{total}} + d_{\text{total}}$); when $D_{\text{total}} = a_{\text{total}} + d_{\text{total}}$; and when $D_{\text{total}} = a_{\text{total}} + d_{\text{total}}$ but V_{max} has not yet been reached.

In Fig. 2, case (a) consists of acceleration, constant velocity, and deceleration segments and is of a trapezoidal shape. Case (b) has only acceleration and deceleration segments because the total movement distance is equal to the sum of the acceleration/deceleration segments. Case (c) is similar to case (b); the only difference is that in (c) the maximum velocity is not reached.

For Fig. 2, at an arbitrary time instant t , the velocity in case (a) can be expressed as

$$V = \begin{cases} at & t_0 \leq t < t_1, \\ V_{\text{max}} & t_1 \leq t < t_2, \\ V_{\text{max}} - a(t - t_2) & t_2 \leq t < t_3, \end{cases} \quad (1)$$

and the velocity in cases (b) and (c) can be expressed as

$$V = \begin{cases} at & t_0 \leq t < t_1, \\ a(t_3 - t) & t_1 \leq t < t_2, \end{cases} \quad (2)$$

where a is the acceleration in cases (b) and (c).

As indicated by Figs. 1 and 2, it is possible to control the motion/velocity of motors in automatic guided vehicles (AGVs) through the relation between the total movement of an

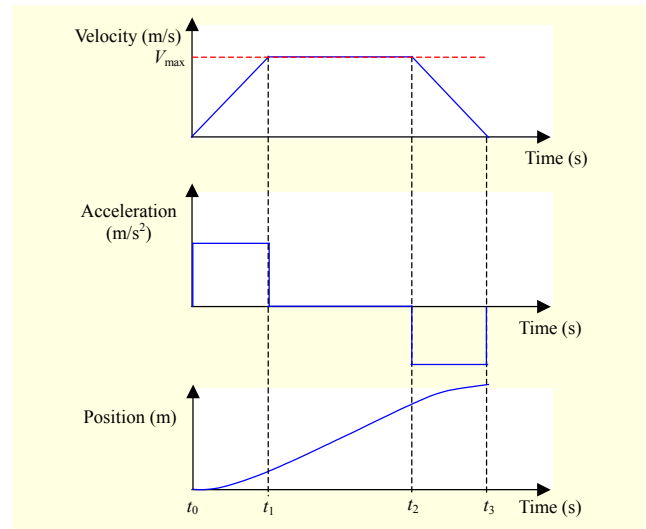


Fig. 1. Trapezoidal velocity profile.

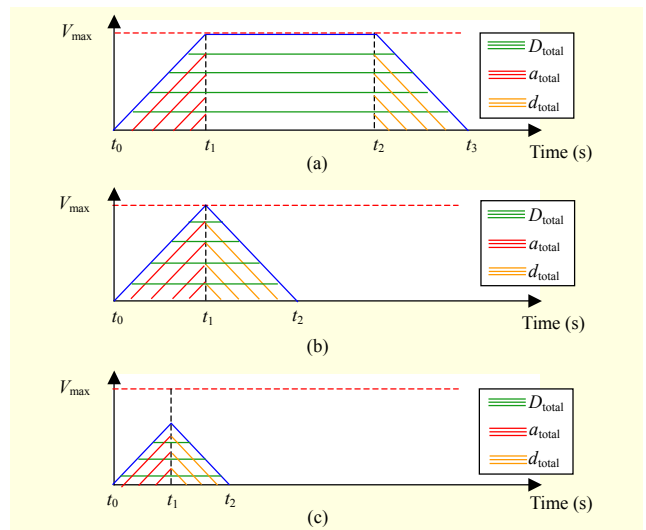


Fig. 2. Velocity profiles in terms of relation between D_{total} and $a_{\text{total}} + d_{\text{total}}$: (a) $D_{\text{total}} > a_{\text{total}} + d_{\text{total}}$, (b) $D_{\text{total}} = a_{\text{total}} + d_{\text{total}}$, and (c) $D_{\text{total}} = a_{\text{total}} + d_{\text{total}}$ but V_{max} has not yet been reached.

object and its acceleration/deceleration. Therefore, trapezoidal velocity profiles have been widely applied to high-accuracy applications, such as motion control, robotics, and so on.

III. Modeling of Velocity Profiles for Infeed Control of Sorting System

1. Infeed Control Process in Sorting System

Figure 3 shows the configuration for the infeed line of a sorting system. The infeed line consists of a measurement conveyor belt, five VCBs, and a transition conveyor belt (TCB). The measurement conveyor belt, which has a constant

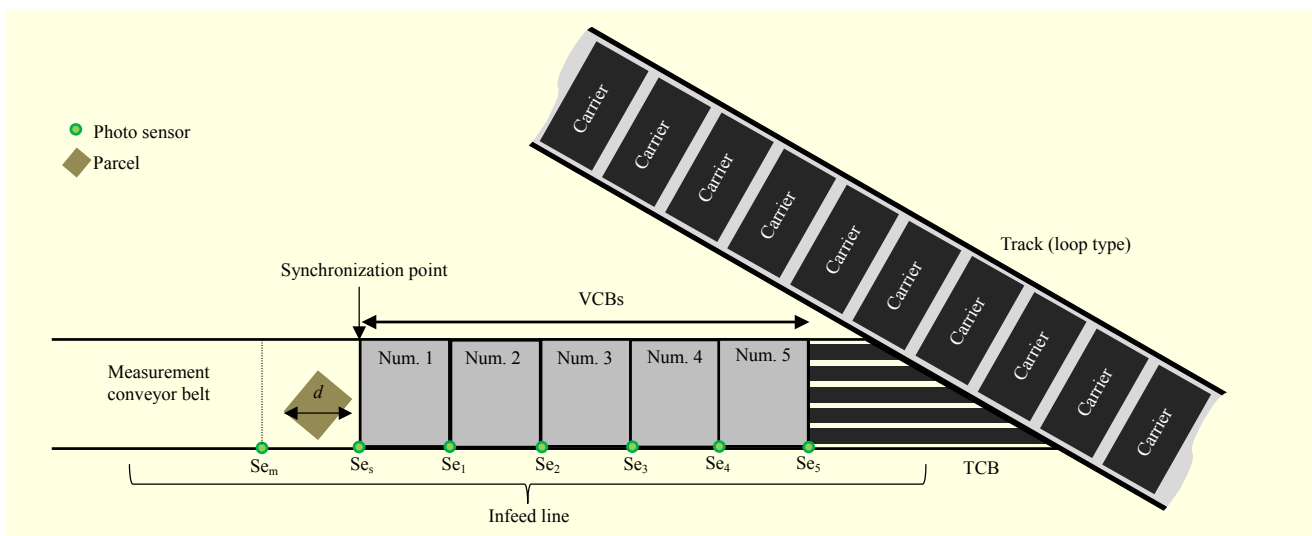


Fig. 3. Configuration for the infeed line of sorting system.

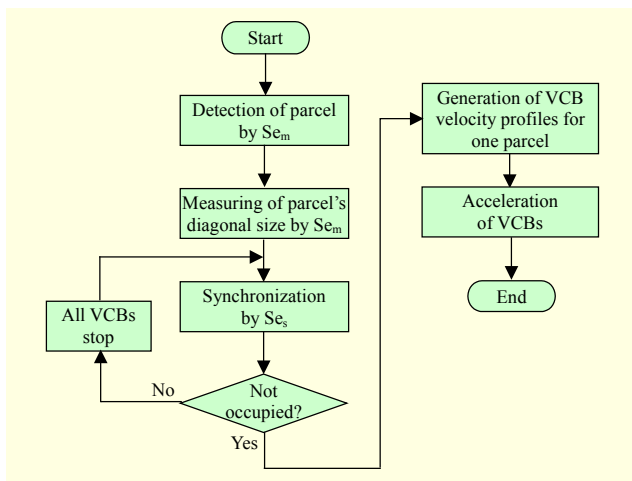


Fig. 4. Flowchart of infeed control for a single parcel.

velocity, is responsible for the measuring of a parcel's diagonal size (top face of parcel) through a photo sensor (Se_m). The VCBs are used to synchronize parcels and track carriers. The TCB, which also has a constant velocity, only moves parcels to track carriers. An encoder system tracks the locations of the track carriers and continuously measures the velocity of the track, which is assumed to be constant. A photo sensor is located at the beginning of each VCB so that the infeed control system knows when a parcel is about to enter a particular VCB. This allows the infeed control system to manage the VCBs' starting times of acceleration/deceleration. Among the three types of conveyor belt, only the VCBs have the ability to accelerate/decelerate; the velocities of the transition and measurement conveyor belts are always constant. It is this ability that enables our system to improve the handling rate of the infeed system.

Figure 4 shows the flowchart for the infeed control process for each infeed parcel. The infeed control starts by detecting a parcel by the sensor Se_m . Synchronization of a parcel and track carrier starts as soon as a parcel is detected by the sensor Se_s . At the same time, the main controller is always monitoring whether the carrier is occupied by a parcel. If there are no available track carriers, then all VCBs come to a halt. When an empty track carrier is available, then all VCBs begin to accelerate once again in accordance with their respective newly generated velocity profiles.

2. Velocity Profile for Single Parcel in Infeed Control of Sorting System

Figure 5 shows the velocity changes for each VCB as a parcel moves along the infeed line in the specific case where the PE of a selected track carrier is set to a value of one (out of twenty nine). The PE value is the remainder after dividing the number of real-time pulses by the number of encoder sensors. Real-time pulses are generated by encoder sensors, which are activated whenever a track carrier passes through them.

Unlike in AGVs where trapezoidal velocity profiles having an initial velocity of zero are used, the VCBs in this system are considered to always have an initial velocity, $V_{initial}$. The sensors (Se_1 to Se_5) located respectively at the end of each of the VCBs (VCB 1 to VCB 5) play a role in detecting the position of the parcel. Just as a parcel has completely left a VCB, the respective VCB immediately begins to decelerate at maximum velocity. The position of the parcel dictates when a VCB will first begin to accelerate. In the figure, VCBs 1 and 2 have the same acceleration starting point; that is, they simultaneously begin to accelerate just as the parcel reaches the location of

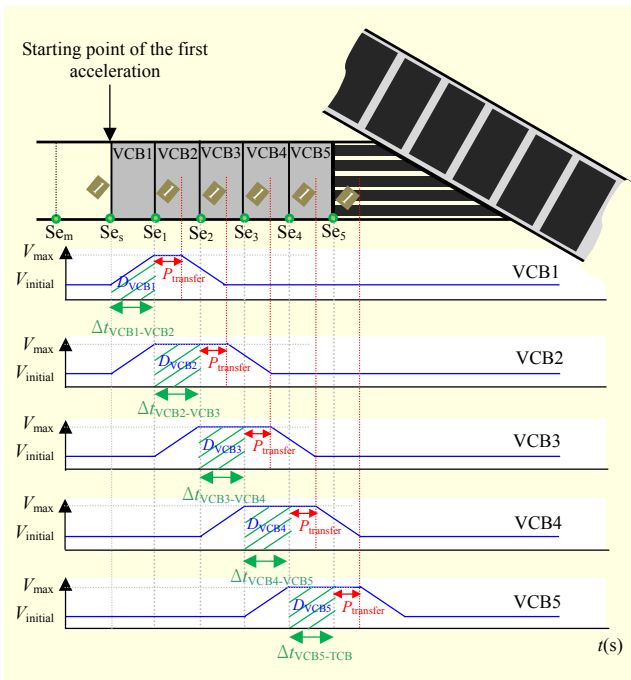


Fig. 5. Each VCB's velocity changes as the parcel moves along the infeed line (position encoder (PE) = 1).

sensor Se_s .

To transfer a parcel from one VCB to the next in a smooth fashion, it is essential that during this *transfer* stage, denoted by $P_{transfer}$ in Fig. 5, the velocities of the parcel-carrying VCB and the receiving VCB be the same throughout this period. In addition, in the figure, the area under the velocity curve represented by D_{VCB1} is the total movement distance of the parcel for that period of time, which equates to the length of VCB 1. Likewise with D_{VCB2} to D_{VCB5} . The period of time from when the parcel first enters VCB 1 until it first enters VCB 2 is denoted by $\Delta t_{VCB[0]_{1-VCB2}}$. Likewise with $\Delta t_{VCB[0]_{2-VCB3}}$, $\Delta t_{VCB[0]_{3-VCB4}}$, and $\Delta t_{VCB[0]_{4-VCB5}}$. The period of time from when the parcel first enters VCB 5 until it first enters the TCB is denoted by $\Delta t_{VCB[0]_{5-TCB}}$.

Figure 6 shows the velocity profiles of VCB 1 for various PE values as a single parcel travels along the infeed line. The starting time of VCB 1's acceleration is represented by $t_{VCB1acc}$. The moment in time when a parcel first enters VCB 1 is denoted by t_{PVCB1} . Likewise with t_{PVCB2} , t_{PVCB3} , t_{PVCB4} , t_{PVCB5} , and t_{PTCB} . The variables $t_{VCB1acc}$, $\Delta t_{VCB[0]_{1-VCB2}}$, and $P_{transfer}$ (the period of time from when the parcel first enters VCB 2 until it has completely left VCB 1) are assigned beforehand according to the real-time positions of track carriers and parcels' diagonal sizes; the real-time positions of track carriers is detected by the PE. Moreover, $t_{VCB1acc}$, $\Delta t_{VCB[0]_{1-VCB2}}$, and $P_{transfer}$ will have to be readjusted whenever the distance between two consecutive parcels is narrow enough to affect the initial velocity of a VCB,

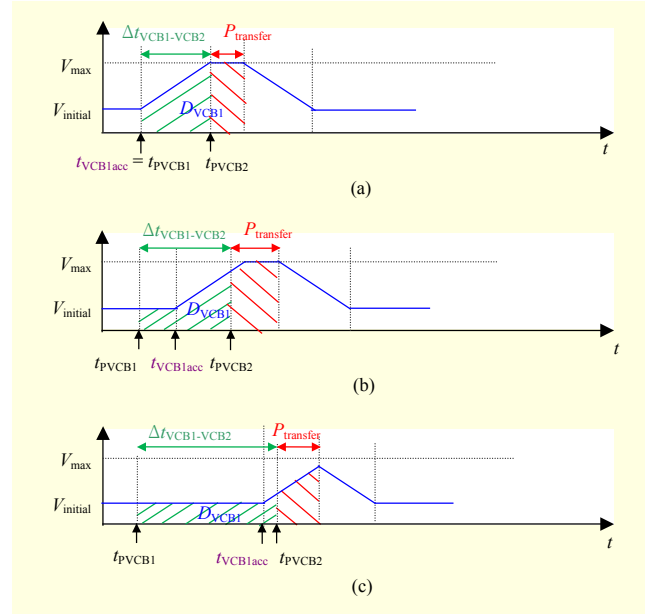


Fig. 6. Velocity profiles of VCB 1 for a single parcel according to various PE values: (a) PE = 1, (b) PE = 10, and (c) PE = 29.

$V_{initial}$. It is this necessary readjustment that leads to the creation of a modified trapezoidal velocity profile, which in turn, ensures that a parcel will be able to synchronize correctly (following the readjustment) with its intended carrier.

The velocity profile of Fig. 6(a), where PE = 1, represents the case where VCB 1 accelerates to V_{max} in the quickest time possible and remains at that velocity for as long as possible; thus, this would mean that the whole system is operating at maximum speed.

Figure 7 shows the velocity profiles of a single parcel according to different PE values. In Figs. 7(a)–(c), the total distance travelled by a parcel along the infeed line from the point Se_m to the end of TCB, D_{total} , is a fixed distance (that is, $D_{total} = (D_{VCB1} + D_{VCB2} + D_{VCB3} + D_{VCB4} + D_{VCB5} + D_{TCB})$). The moment in time when the parcel first enters its intended track carrier is denoted by t_{Final} . The total movement time of a parcel (Δt_{PE}) and acceleration starting time of VCB 1 ($t_{VCB1acc}$) are assigned according to the PE value. The total distance travelled by a parcel along the infeed line, D_{total} , in Figs. 7(a), (b), and (c) is given by

$$D_{total} = \int_{t_{PVCB1}}^{t_{Final}} V(t) dt = \int_{t_{PVCB1}}^{t_{VCB1acc}} V_1(t) dt + \int_{t_{VCB1acc}}^{t_{Vmax}} V_2(t) dt + \int_{t_{Vmax}}^{t_{Final}} V_3(t) dt, \quad (3)$$

where V_1 is the velocity of the parcel during t_{PVCB1} to $t_{VCB1acc}$, V_2 is the velocity of the parcel during $t_{VCB1acc}$ to t_{Vmax} , and V_3 is the velocity of the parcel during t_{Vmax} to t_{Final} ; t_{Vmax} is the moment in time when the parcel reaches V_{max} . In the cases where $t_{PVCB1} =$

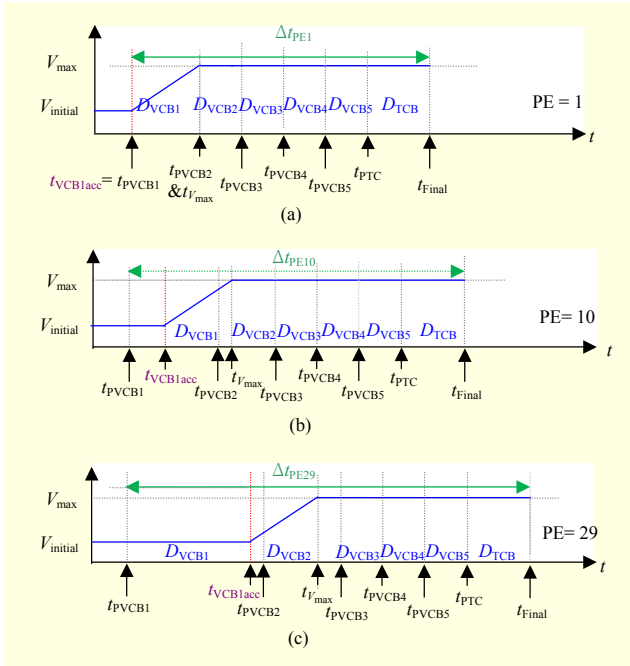


Fig. 7. Velocity profiles of a single parcel according to various PE values.

0 and where a parcel experiences no acceleration during $t_{PVCB1} \leq t \leq t_{VCB1acc}$ and $t_{Vmax} \leq t \leq t_{Final}$, V_1 , V_2 , and V_3 can, respectively, be expressed as follows:

$$\begin{aligned} V_1(t) &= V_{initial}, \\ V_2(t) &= V_{initial} + at, \\ V_3(t) &= V_{max}. \end{aligned} \quad (4)$$

Thus, using (4), (3) can be expressed as follows:

$$\begin{aligned} D_{total} &= V_{initial}t_{VCB1acc} + V_{initial}t_{Vmax} + \frac{at_{Vmax}^2}{2} - V_{initial}t_{VCB1acc} \\ &\quad - at_{VCB1acc}^2 + V_{max}t_{Final} - V_{max}t_{Vmax} \\ &= V_{initial}t_{Vmax} + \frac{a(t_{Vmax} - t_{VCB1acc})^2}{2} + V_{max}(t_{Final} - t_{Vmax}). \end{aligned} \quad (5)$$

Multiplying both sides of (5) by two and simplifying, we obtain the following:

$$\begin{aligned} 2D_{total} &= 2V_{initial}t_{Vmax} + a(t_{Vmax} - t_{VCB1acc})^2 + 2V_{max}(\Delta t_{PE} - t_{Vmax}) \\ 0 &= 2V_{initial}t_{Vmax} + a(t_{Vmax} - t_{VCB1acc})^2 + 2V_{max}(\Delta t_{PE} - t_{Vmax}) \\ &\quad - 2D_{total} \\ 0 &= at_{VCB1acc}^2 - 2at_{Vmax}t_{VCB1acc} + 2V_{initial}t_{Vmax} + at_{Vmax}^2 \\ &\quad + 2V_{max}(\Delta t_{PE} - t_{Vmax}) - 2D_{total}, \end{aligned} \quad (6)$$

where $t_{Final} = \Delta t_{PE}$. In (6), Δt_{PE} is determined by means of PE. By replacing “ $2V_{initial}t_{Vmax} + at_{Vmax}^2 + 2V_{max}(\Delta t_{PE} - t_{Vmax}) - 2D_{total}$ ” with “ C ,” we can reduce (6) to the following quadratic function:

$$at_{VCB1acc}^2 - 2at_{Vmax}t_{VCB1acc} + C = 0. \quad (7)$$

Thus, (7) can be solved to give the following solutions for $t_{VCB1acc}$:

$$t_{VCB1acc} = \frac{2at_{Vmax} \pm \sqrt{(-2at_{Vmax})^2 - 4aC}}{2a}. \quad (8)$$

In (8), t_{Vmax} is a constant determined by $(V_{initial} + V_{max})/a$. However, $t_{VCB1acc}$ needs to be altered if the distance between the first and second parcels is narrow enough to affect $V_{initial}$. If such an event arises, then this can lead to inaccurate infeed control or failure of synchronization between the second parcel and its intended track carrier. This problem is analyzed in the next section.

3. Two Parcels with Narrow Interval

Figure 8 shows how $\Delta t_{VCB[0]1-VCB2}$ and $V_{initial}$ can change in accordance with the value of “ $VCB_{width} + \Delta I$ ” in the case where $PE = 1$ for both the first and second parcels. The variable VCB_{width} , as its name suggests, represents the width of one of the VCBs (all VCBs are of the same width). To control multiple parcels individually, it is a necessary condition that only one parcel exist on a VCB at any given time. Given this condition, the minimum permitted distance between two parcels is VCB_{width} . In reality, it is extremely unlikely that multiple parcels will enter the infeed line at exactly a distance of VCB_{width} between them. Therefore, the distance between two consecutive parcels entering the infeed line is modeled by “ $VCB_{width} + \Delta I$,” where ΔI is some variable additional distance beyond that of the minimum permitted (VCB_{width}).

Figure 8(b) shows the velocity profile of VCB 1 for the first parcel when $PE = 1$. Figure 8(c) shows the velocity profile of VCB 1 for the second parcel in the case of $\Delta I = 0$, where V_x is the velocity of VCB 1 at t_{PVCB1} of the second parcel. In other words, the second parcel begins to move onto VCB 1 as soon as the first parcel has completely left VCB 1. Figure 8(d) shows the velocity profile of VCB 1 for the second parcel in the case of $\Delta I = 35$ cm. Figure 8(e) shows the velocity profile of VCB 1 for the second parcel in the case of $\Delta I = 70$ cm. Figure 8(e) shows that $\Delta t_{VCB[0]1-VCB2}$ and $V_{initial}$ of the second parcel are unaffected by “ $VCB_{width} + \Delta I$.” Hence, it is not necessary to create a modified velocity profile for the second parcel. This parcel will simply move along the infeed line using the velocity profile associated with its PE value at the time.

In Fig. 8(b), the interval ΔI without changing $\Delta t_{VCB[0]1-VCB2}$ and $V_{initial}$ of the second parcel is given by

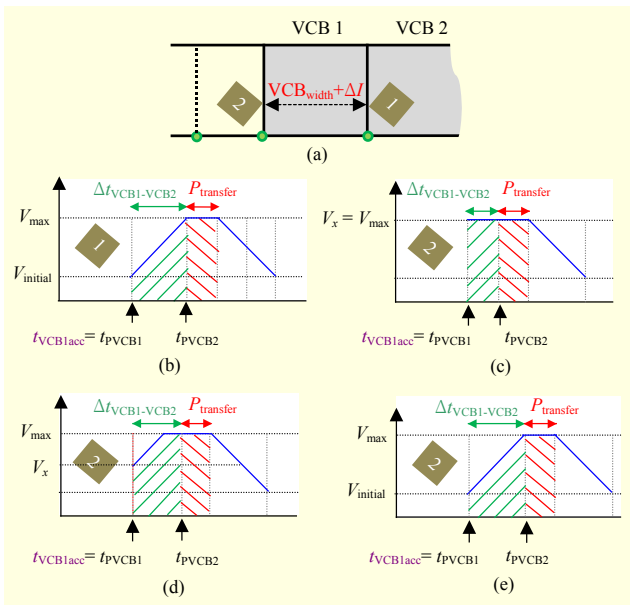


Fig. 8. Changes in $\Delta t_{VCB1-VCB2}$ according to the interval between two parcels: (a) distance between parcel 1 and parcel 2; (b) velocity profile of VCB 1 for parcel 1 with PE = 1; and (c)–(e) velocity profiles of VCB 1 for parcel 2 with PE = 1, where each “ $VCB_{width} + \Delta I$ ” is about 70 cm, 105 cm, and 140 cm, respectively.

$$\begin{aligned}
 \Delta I &= \int_{t_{PVCB1}}^{t_{PVCB2}} V(t) dt \\
 &= V_{initial} (t_{PVCB2} - t_{PVCB1}) + \frac{a(t_{PVCB2} - t_{PVCB1})^2}{2} \\
 &= V_{initial} t_{PVCB2} - V_{initial} t_{PVCB1} + \frac{a(t_{PVCB2} - t_{PVCB1})^2}{2} \\
 &= V_{initial} t_{PVCB2} + \frac{a(t_{PVCB2})^2}{2},
 \end{aligned} \tag{9}$$

where V_{max} is 2.9 m/s and a is 4.6 m/s². The time t_{PVCB2} is given by $(V_{max} - V_{initial})/a$, where $V_{initial}$ is 1.4 m/s. By inserting the values from $V_{initial}$, a , and t_{PVCB2} into (9), the interval ΔI without changing $\Delta t_{VCB}[0]_{1-VCB2}$ and $V_{initial}$ of the second parcel should be more than 70 cm. As shown in Figs. 8(c) and 8(d), a narrow interval among parcels leads to a change in the values of $\Delta t_{VCB}[0]_{1-VCB2}$ and $V_{initial}$ for the second parcel. This can cause a change in the total movement time Δt_{PE} of the second parcel, which in turn, would mean that the parcel would fail to synchronize correctly with its intended track carrier.

In our study, there are 29 possible PE values, which means that the total movement time Δt_{PE} of a parcel will correspond to one of these values. This is true of all parcels passing through the system — each will have its own Δt_{PE} value that corresponds to one of 29 possible PE values. However, the Δt_{PE} of the second parcel is dependent upon the interval “ $VCB_{width} + \Delta I$ ” and its size. If $70 \text{ cm} \leq VCB_{width} + \Delta I \leq 140 \text{ cm}$, then the

resulting change to Δt_{PE} of the second parcel leads to the creation of a time error, Δt_e . The time error Δt_e is generated when $\Delta t_{VCB}[0]_{1-VCB2}$ and $V_{initial}$ of the second parcel are changed. The Δt_e of the second parcel indicates that the second parcel will fail to synchronize correctly with its intended track carrier; hence, a modified velocity profile for the second parcel will have to be created accordingly.

4. Modified Velocity Profile for Two Parcels with Narrow Interval

In the cases of two or more parcels, where the interval between any two consecutive parcels is $70 \text{ cm} \leq VCB_{width} + \Delta I \leq 140 \text{ cm}$, it is necessary to model a modified velocity profile to accurately synchronize the parcels with their intended track carriers. Figure 9 shows an infeed control model using a modified velocity profile. In this infeed control model, the inputs are the interval between two consecutive parcels (“ $VCB_{width} + \Delta I$ ”), a parcel’s diagonal size (d), and the PE value. Using these inputs, a controller is able to then generate a modified velocity profile and determine $t_{VCB1acc}$ and Δt_{PE} in advance. The controller decides the type of velocity profile by means of the following factors:

- “ $VCB_{width} + \Delta I$,” where “ VCB_{width} ” is the minimum acceptable distance between parcels.
- Δt_{PE} by PE of the first parcel.
- Δt_{PE} by PE of the second parcel.
- The value of t_{PVCB1} for the second parcel.

Figure 10 shows the velocity profiles of the second parcel under the assumption that PE = 1 for both the first and second parcels, in the cases where $\Delta I = 0$ and $\Delta I \geq 70 \text{ cm}$. Figure 10(b) shows the velocity profile of the second parcel in the case where the distance between the first and second parcels is greater than 140 cm. In other words, this velocity profile indicates that the first parcel has no effect on the velocity profile of the second due to the fact that $\Delta I \geq 70 \text{ cm}$. Figure 10(c) shows the velocity profile of the second parcel in the case where $\Delta I = 0$. This velocity profile generates a time error, Δt_e , which indicates that the second parcel will not synchronize correctly with its intended track carrier. As shown in Fig. 10(c), the interval $\Delta I < 70 \text{ cm}$ leads to a change

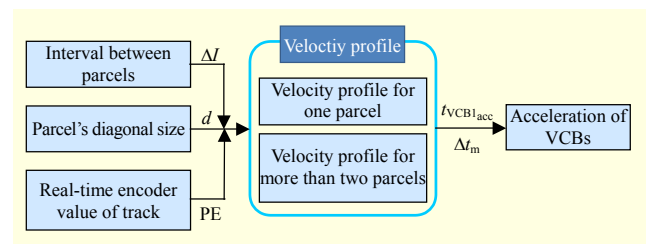


Fig. 9. Infeed control model using modified velocity profile.

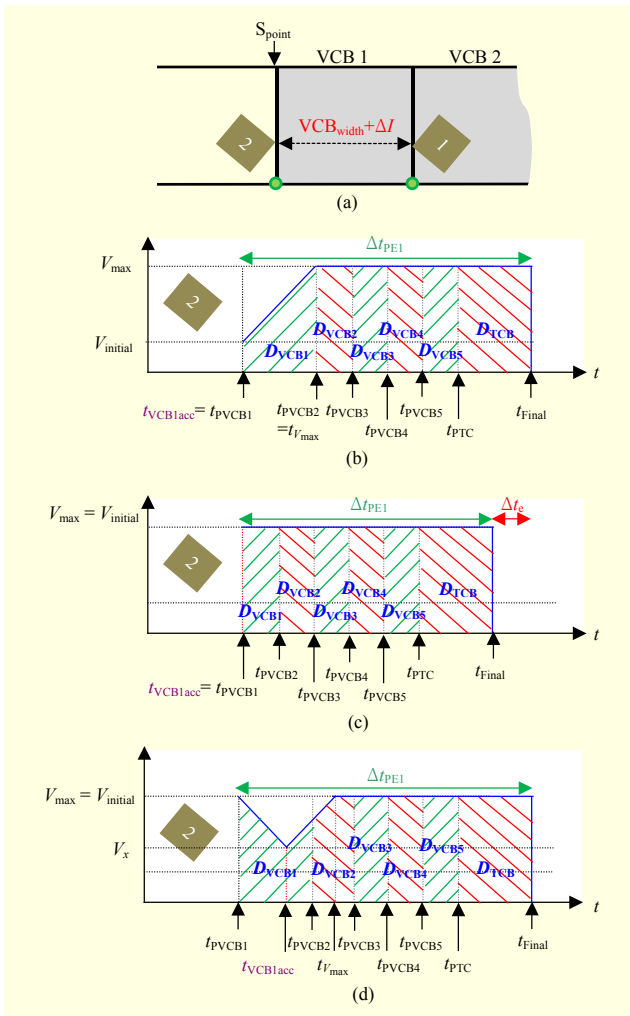


Fig. 10. Velocity profiles of the second parcel in the case where PE = 1 for both parcels: (a) interval between parcels; (b) velocity profile of the second parcel when $\Delta I \geq 70$ cm; (c) velocity profile of the second parcel when $\Delta I = 0$ cm; and (d) modified velocity profile for the second parcel to offset Δt_e .

in the original Δt_{PE} .

Figure 10(d) is the modified velocity profile of the second parcel, which is created in such a way so as to offset Δt_e . The starting time of the acceleration for VCB1, $t_{VCB1acc}$, is the most important factor because the original Δt_{PE} can be optimized by $t_{VCB1acc}$. In Fig. 10(d), the total movement distance D_{total} is given by

$$D_{total} = \int_{t_{PVCB1}}^{t_{Final}} V(t) dt = \int_{t_{PVCB1}}^{t_{VCB1acc}} V_1(t) dt + \int_{t_{VCB1acc}}^{t_{V_{max}}} V_2(t) dt + \int_{t_{V_{max}}}^{t_{Final}} V_3(t) dt, \quad (10)$$

where $t_{PVCB1} = 0$ and $a = 0$ ($t_{V_{max}} \leq t \leq t_{Final}$). Therefore, V_1 , V_2 , and V_3 are expressed, respectively, as follows:

$$\begin{aligned} V_1(t) &= V_{max} - at, \\ V_2(t) &= V_x + at, \\ V_3(t) &= V_{max}. \end{aligned} \quad (11)$$

Equations (10) and (11) can be expressed as follows:

$$\begin{aligned} D_{total} &= V_{max} t_{VCB1acc} - \frac{at_{VCB1acc}^2}{2} + V_x t_{V_{max}} + \frac{at_{V_{max}}^2}{2} \\ &\quad - \left(V_x t_{VCB1acc} + \frac{at_{VCB1acc}^2}{2} \right) + V_{max} t_{VCB1acc} - V_{max} t_{V_{max}} \\ &= at_{VCB1acc}^2 - t_{VCB1acc} (V_{max} - V_x) - \frac{at_{V_{max}}^2}{2} \\ &\quad + t_{V_{max}} (V_{max} - V_x) - V_{max} t_{Final}. \end{aligned} \quad (12)$$

In Fig. 10(d), we can obtain the relation of $2t_{VCB1acc} = t_{V_{max}}$ because the acceleration time of VCBs is equal to the deceleration time of those. The relation of V_x and $t_{VCB1acc}$ is as follows:

$$V_x = V_{max} - at_{VCB1acc}. \quad (13)$$

By inserting $t_{V_{max}} = 2t_{VCB1acc}$, $t_{Final} = \Delta t_{PE}$, and $V_x = V_{max} - at_{VCB1acc}$ into (12), we obtain the following:

$$at_{VCB1acc}^2 + V_{max} \Delta t_{PE} - D_{total} = 0. \quad (14)$$

Then, (14) can be solved to give

$$t_{VCB1acc} = \frac{\pm \sqrt{-4a(V_{max} \Delta t_{PE} - D_{total})}}{2a}. \quad (15)$$

In (15), Δt_{PE} is assigned according to the PE value. The values a , D_{total} , and V_{max} are constant regardless of PE or ΔI . Therefore, a modified velocity profile can be generated from the derived $t_{VCB1acc}$ so as to correctly synchronize a parcel with its intended track carrier.

IV. Experimental Results

To verify the use of modified velocity profiles in the infeed control, experiments are conducted on a cross-belt-type sorting system (model name: SCS 1500) manufactured by Vanderlande Industries. The specifications of the cross-belt-type sorting system are as follows:

- Track velocity, V_T , is equal to 2.5 m/s.
- Carrier width is 800 mm.
- Infeed line consists of one measurement belt, five variable belts, and one transition belt.
- $V_{max} = 2.9$ m/s and $V_{initial} = 1.4$ m/s.
- A VCB's rate of acceleration or deceleration is constant at 4.6 m/s².

Figure 11 shows the configuration of a parcel and carrier for the purposes of experiment. In the figure, W is the width of the

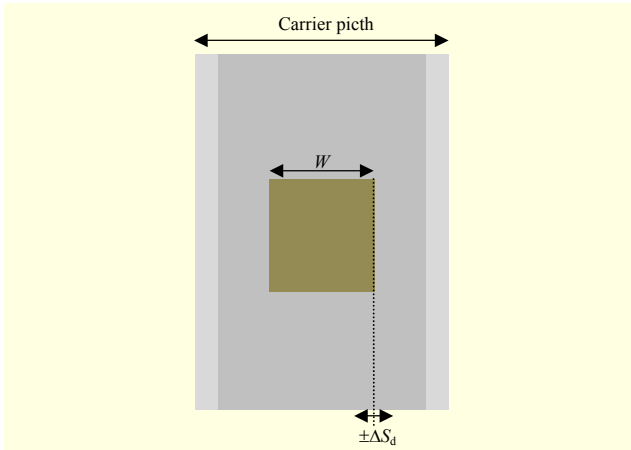


Fig. 11. Configuration of parcel and carrier for experiment.



Fig. 12. Picture of sorting system's infeed line used in experiments.

parcel and ΔS_d is the indicator judging success or failure for synchronization between the parcel and its intended track carrier. In other words, ΔS_d indicates how far the center of the parcel is from the center of the carrier. Figure 12 shows a picture of an infeed line of the sorting system used in the experiment. Figure 13 shows the changes in ΔS_d in terms of ΔI before applying the proposed algorithm. The experiment conditions are as follows:

- The PE of the first parcel is fixed at a value of one.
- The PE of the second parcel is varied (PE = 1, PE = 14, and PE = 29).
- ΔI ranges from 0 cm to 70 cm.

As can be seen from Fig. 13, the larger the value of ΔI , the smaller ΔS_d becomes. A stable synchronization between a second parcel and its intended track carrier can be achieved when ΔI is greater than 70 cm.

Figure 14 shows the changes in ΔS_d in terms of ΔI before applying the proposed infeed control algorithm. The experimental conditions are the same as those for Fig. 13, except that the PE of the first parcel is fixed now at a value of

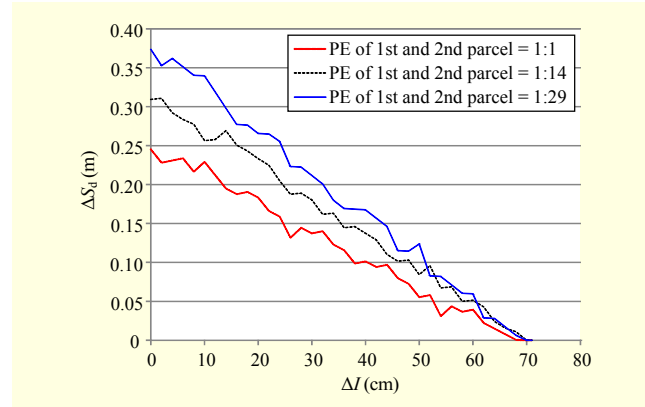


Fig. 13. ΔS_d in terms of ΔI before applying proposed algorithm: first parcel's PE value is always set at one. Second parcel's PE value is varied (PE = 1, PE = 14, and PE = 29).

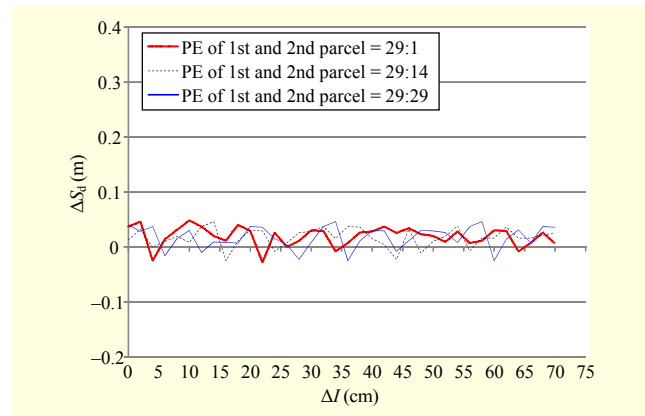


Fig. 14. ΔS_d in terms of ΔI before applying proposed algorithm: first parcel's PE value is always set at 29. Second parcel's PE value is varied (PE = 1, PE = 14, and PE = 29).

29. As shown in Fig. 14, the range of values for ΔS_d indicates the success for synchronization between the second parcel and its intended track carrier. Although there is a slight acceleration of VCB1 for the first parcel when PE = 29, ΔS_d is within the tolerance range. Figure 15 indicates the changes in ΔS_d in terms of ΔI after applying the proposed algorithm. The experiment conditions are the same as those for Fig. 13, except that the modified velocity profile is applied to offset the time error Δt_e .

As shown in Fig. 16, to verify the infeed capacity of one infeed line by mathematics and a field test, the following conditions are introduced:

- " $VCB_{width} + \Delta P$ " is about 140 cm if the proposed algorithm is not used.
- " $VCB_{width} + \Delta P$ " is about 70 cm if the proposed algorithm is used.
- A parcel's width is about 40 cm.
- V_a is set at 2.7 m/s.

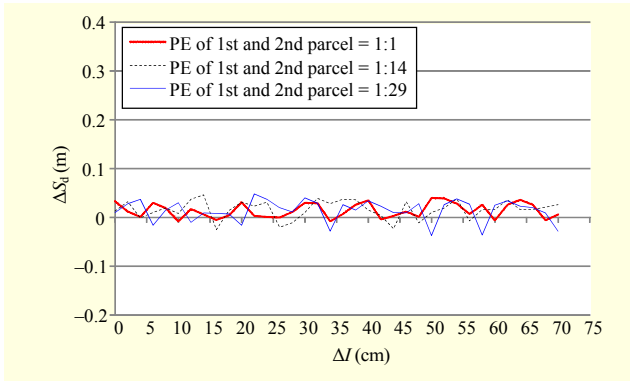


Fig. 15. ΔS_d in terms of ΔI after applying proposed algorithm: first parcel's PE value is always set at 1. Second parcel's PE value is varied (PE = 1, PE = 14, and PE = 29).

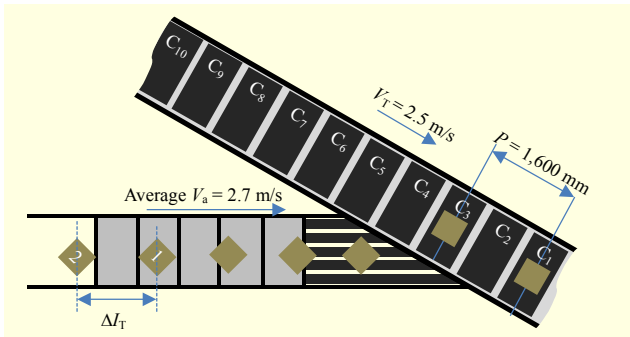


Fig. 16. Configuration of field test for performance of one infeed line.

The infeed capacity per hour for a sorting system is given by

$$\text{Infeed capacity} = \frac{V_T \times 3,600}{P}, \quad (16)$$

where V_T is the track's speed (2.5 m/s) and P is the distance between the centers of two carriers having parcels. In the case where each carrier is occupied by a single parcel, the infeed capacity is maximized at 11,250 per hour. In the case where every other carrier is occupied by a parcel, the infeed capacity is reduced to 5,625 per hour. In other words, P becomes 160 cm. In (16), the infeed capacity is determined by the value of P . The value of P can be changed by (17) below

$$P = \frac{\Delta I_T \times V_T}{V_a}, \quad (17)$$

where V_a is the average speed of the five VCBs and transition belt and ΔI_T is the distance between the centers of two consecutive parcels. In addition, the conditions in (18) below are applied for stable infeed.

$$\begin{aligned} 0 \text{ m} < P \leq 0.8 \text{ m} : P &= 0.8 \text{ m}, \\ 0.8 \text{ m} < P \leq 1.6 \text{ m} : P &= 1.6 \text{ m}, \\ 1.6 \text{ m} < P \leq 2.4 \text{ m} : P &= 2.4 \text{ m}. \end{aligned} \quad (18)$$

In (17) and (18), P is 2.4 m under the following conditions:

- The proposed algorithm is not used.
- ΔI_T is about 1.964 m and “VCB_{width} + ΔP ” is 1.4 m ($\Delta I = 0.7$ m).

As a result, the infeed capacity per hour is 3,750 parcels. In addition, P is 1.6 m under the following conditions:

- The proposed algorithm is applied.
- ΔI_T is about 1.264 m and “VCB_{width} + ΔP ” is 0.7 m ($\Delta I = 0$ m).

Consequently, the infeed capacity per hour is 5,625 parcels.

Field tests to measure the infeed capacity are implemented with the cross-belt-type sorting system installed at a Korea Post mail distribution center. The infeed capacity without applying the proposed algorithm is around 4,000 parcels per hour. The infeed capacity with the proposed algorithm applied is around 5,600 parcels per hour. However, there are some discrepancies between the mathematics and field test results. This is because V_a in the field test is a variable value from 1.4 m/s to 2.9 m/s depending on the value of PE.

V. Conclusion

This paper explained how modified trapezoidal velocity profiles are applied to the infeed control algorithm of a parcel sorting system. The proposed algorithm can eliminate the time error Δt_e , which is generated by the narrow interval ΔI and lower PE values of the first parcel. To be specific, Δt_{PE} is derived through a mathematical modeling of the acceleration starting time of VCB 1, $t_{VCB1acc}$.

To validate the use of modified velocity profiles, a cross-belt-type sorting system (model name: SCS 1500) manufactured by Vanderlande Industries is used. Under the proposed method, synchronization between a parcel and its intended track carrier is accurately achieved. In addition, the performance of an infeed line can be improved by up to 40%, at a rate of 5,600 items/hr. This improvement in performance means that it may well be possible to reduce the required number of infeed lines for a parcel sorting system; hence maximizing the sorting system's performance.

References

- [1] J.U. Cho and J.W. Jeon, “A Motion-Control Chip to Generate Velocity Profiles of Desired Characteristics,” *ETRI J.*, vol. 27, no. 5, Oct. 2005, pp. 563–568.
- [2] H.Z. Li et al., “A New Motion Control Approach for Jerk and Transient Vibration Suppression,” *IEEE Int. Conf. Ind. Informat.*, Singapore, Aug. 16–18, 2006, pp. 676–681.
- [3] S.-Y. Lee et al., “S-Curve Profile Switching Method Using Fuzzy System for Position Control of DC Motor Under Uncertain

Load,” *IEEE Int. Conf. Contr., Autom. Syst.*, Jeju, Rep. of Korea, Oct. 17–21, 2012, pp. 91–95.

- [4] F.-J. Lin, K.-K. Shyu, and C.-H. Lin, “Incremental Motion Control of Linear Synchronous Motor,” *IEEE Trans. Aerosp. Electron. Syst.*, vol. 38, no. 3, July 2002, pp. 1011–1022.
- [5] H. Li et al., “Design of Global Sliding-Mode Controlled AC Servo Controller Based on Exponential Acceleration/Deceleration Algorithm,” *Int. Conf. Mechatronics Autom.*, Xi’an, China, Aug. 4–7, 2010, pp. 1507–1511.
- [6] M. Haddad, W. Khalil, and H.E. Lehtihet, “Trajectory Planning of Unicycle Mobile Robots with a Trapezoidal-Velocity Constraint,” *IEEE Trans. Robot.*, vol. 26, no. 5, Oct. 2010, pp. 954–962.
- [7] K.-H. Rew and K.-S. Kim, “A Closed-Form Solution to Asymmetric Motion Profile Allowing Acceleration Manipulation,” *IEEE Trans. Ind. Electron.*, vol. 57, no. 7, July 2010, pp. 2499–2506.
- [8] Z. Rymansaib, P. Iravani, and M.N. Sahinkaya, “Exponential Trajectory Generation for Point to Point Motions,” *IEEE/ASME Int. Conf. Adv. Intell. Mechatronics*, Wollongong, Australia, July 9–12, 2013, pp. 906–911.
- [9] Y. Wang, J. Li, and Z. Li, “An Advanced Velocity Profiles Optimizes Approach for CNC Machine Tools,” *Int. Conf. Digital Manuf. Autom.*, Changsha, China, Dec. 18–20, 2010, pp. 172–175.
- [10] U. Naoki, H. Yuta, and S. Shigenori, “Residual Vibration Suppression and Energy Saving in Industrial Machines Using a Trapezoidal Velocity Profile,” *American Contr. Conf.*, Portland, OR, USA, June 4–6, 2014, pp. 323–328.
- [11] T. Chettibi et al., “Suboptimal Trajectory Generation for Industrial Robots Using Trapezoidal Velocity Profiles,” *IEEE/RSJ Int. Conf. Intell. Robots Syst.*, Beijing, China, Oct. 2006, pp. 729–735.
- [12] S. Thirachai et al., “Trapezoidal Velocity Trajectory Generator with Speed Override Capability,” *Int. Conf. Contr. Autom. Syst.*, Ilsan, Rep. of Korea, Oct. 27–30, 2010, pp. 1468–1472.
- [13] SCS 1500 by Vanderlande Industries, 2012. Accessed Feb. 15, 2012. <http://www.vanderlande.com>



Ki Hak Kim received his BS degree in electronics from Dong-A University, Busan, Rep. of Korea, in 2004 and his MS degree in electronics from the Information and Communications University, Daejeon, Rep. of Korea, in 2006. Since 2006, he has been working for the Electronics and Telecommunications Research Institute, Daejeon, Rep. of Korea, where he is now a senior member of the researching staff. His main research interests are automatic control, system control, RF systems, UWB antenna, and RFID.



Yong Hoon Choi received his BS degree in mechanical engineering from the University of Ulsan, Rep. of Korea, in 1997 and his MS and PhD degrees in industrial and manufacturing systems engineering from Iowa State University, Ames, USA, in 1999 and 2003, respectively. Since 2004, he has been working for the Electronics and Telecommunications Research Institute, Daejeon, Rep. of Korea, where he is now a director of the Logistics Process Research Team. His main research interests are signal processing; process design and monitoring; SCM; and logistics automation.



Hoon Jung received his BS degree in industrial engineering from Kyunghee University, Seoul, Rep. of Korea, in 1989 and his MS and PhD degrees in industrial engineering from Iowa State University, USA and the University of Missouri, USA, in 1997 and 2001, respectively. Since 2002, he has been working for the Electronics and Telecommunications Research Institute, Daejeon, Rep. of Korea, where he is now a senior researcher. His main research interests are supply chain management, logistics information systems, and logistics strategy.